

JOURNAL OF MECHANICAL ENGINEERING

An International Journal

VOLUME 14 NO. 1

JUNE 2017 / ISSN 1823-5514



JOURNAL OF MECHANICAL ENGINEERING

An International Journal

EDITOR IN CHIEF:

Professor Wahyu Kuntjoro – Universiti Teknologi MARA, Malaysia

EDITORIAL BOARD:

Dr. Ahmad Azlan Mat Isa – Universiti Teknologi MARA, Malaysia

Dr. Faqir Gul – Institute Technology Brunei, Brunei Darussalam

Dr. Mohd. Afian Omar – SIRIM Malaysia

Dr. Valliyappan David a/l Natarajan – Universiti Teknologi MARA, Malaysia

Dr. Yongki Go Tiauw Hiong – Florida Institute of Technology, USA

Professor Abdelmagid Salem Hamouda – Qatar University, Qatar

Professor Abdul Rahman Omar – Universiti Teknologi MARA, Malaysia

Professor Bernd Schwarze – University of Applied Science, Osnabrueck, Germany

Professor Bodo Heimann – Leibniz University of Hannover Germany

Professor Darius Gnanaraj Solomon – Karunya University, India

Professor Hazizan Md. Akil – Universiti Sains Malaysia, Malaysia

Professor Mohd. Zulkifly Abdullah – Universiti Sains Malaysia, Malaysia

Professor Roslan Abd. Rahman – Universiti Teknologi Malaysia, Malaysia

Professor Salmiah Kasolang – Universiti Teknologi MARA, Malaysia

Professor Essam E. Khalil – University of Cairo, Egypt

Professor Ichsan S. Putra – Bandung Institute of Technology, Indonesia

Professor Shahrir Abdullah – Universiti Kebangsaan Malaysia

Professor Shahrum Abdullah – Universiti Kebangsaan Malaysia

Professor Masahiro Ohka – Nagoya University, Japan

Professor Mirosław L. Wyszynski – University of Birmingham, UK

Professor P. N. Rao – University of Northern Iowa, USA

Professor Wirachman Wisnoe – Universiti Teknologi MARA, Malaysia

Professor Yongtae Do – Daegu University, Korea

EDITORIAL EXECUTIVES:

Dr. Siti Mariam Abdul Rahman

Dr. Baljit Singh A/L Bathal Singh

Dr. Muhad Rozi Mat Nawi

Dr. Mohd Faizal bin Mohamad

Dr. Noor Azlina Mohd Salleh

Dr. Kausalyah A/P Venkatasoon

Nurul Muthmainnah Mohd Noor

Ahsana Aqilah Ahmad

Rosnadiyah Bahsan

© UiTM Press, UiTM 2017

ISSN 1823-5514

All rights reserved. No part of this publication may be reproduced, stored in a retrieval system, or transmitted in any form or any means, electronic, mechanical, photocopying, recording or otherwise, without prior permission, in writing, from the publisher.

The views, opinions and technical recommendations expressed herein are those of individual researchers and authors and do not necessarily reflect the views of the Faculty or the University.

JOURNAL OF MECHANICAL ENGINEERING

An International Journal

Vol. 14 (1)	June 2017	ISSN 1823-5514	eISSN 2550-164X
-------------	-----------	----------------	-----------------

- 1 Thin-Walled Box Beam Bending Distortion Analytical Analysis 1
A Halim Kadarman
Solehuddin Shuib
Ahmad Yusoff Hassan
Muhammad Adib Izzuddin Ahmad Zahrol
- 2 An Experimental and Theoretical Analysis of Projectile and Target 19
Geometry Effects on Ballistic Limit Velocity
M. Amiri
- 3 A Comparative Study of Prediction Techniques for Supersonic Missile 35
Aerodynamic Coefficients
Loai A. El-Mahdy
Mahmoud Y. M. Ahmed
Osama K. Mahmoud
Omar E. Abdel-Hameed
- 4 Experimental Investigation on the Influences of Varying Injection 61
Timing on the Performance of a B20 JOME Biodiesel Fueled Diesel
Engine
S. Jaichandar
K. Annamalai
- 5 Tensile Performance of Half-Lap Timber Nailed Joint Strengthened 81
using CFRP Sheet
Nurain Rosdi
Nik Norhafiza Nik Yahya
Rohana Hassan
Mohd Hanafie Yasin
Nor Jihan Abd Malek

JOURNAL OF MECHANICAL ENGINEERING

An International Journal

Vol. 14 (1)	June 2017	ISSN 1823-5514	eISSN 2550-164X
-------------	-----------	----------------	-----------------

- 1 Thin-Walled Box Beam Bending Distortion Analytical Analysis 1
A Halim Kadarman
Solehuddin Shuib
Ahmad Yusoff Hassan
Muhammad Adib Izzuddin Ahmad Zahrol
- 2 An Experimental and Theoretical Analysis of Projectile and Target 19
Geometry Effects on Ballistic Limit Velocity
M. Amiri
- 3 A Comparative Study of Prediction Techniques for Supersonic Missile 35
Aerodynamic Coefficients
Loai A. El-Mahdy
Mahmoud Y. M. Ahmed
Osama K. Mahmoud
Omar E. Abdel-Hameed
- 4 Experimental Investigation on the Influences of Varying Injection 61
Timing on the Performance of a B20 JOME Biodiesel Fueled Diesel
Engine
S. Jaichandar
K. Annamalai
- 5 Tensile Performance of Half-Lap Timber Nailed Joint Strengthened 81
using CFRP Sheet
Nurain Rosdi
Nik Norhafiza Nik Yahya
Rohana Hassan
Mohd Hanafie Yasin
Nor Jihan Abd Malek

- 6 Surface Roughness and Roundness Optimization on Turning Process of Aluminium Alloy with Taguchi Method 97
Sudjatmiko
Rudy Soenoko
Agus Suprpto
Moch. Agus Choiron
- 7 Numerical Simulation of the Femur Fracture with and without Prosthesis Under Static Loading using Extended Finite Element Method (X-FEM) 109
Zagane Mohammed El Sallah
Benbarek Ismail
Benouis Ali
Sahli Abderahmen
Bachir Bouiadjra Bel Abbas
Boualem Serier
- 8 Optimization of Robot Plasma Coating Efficiency using Genetic Algorithm and Neural Networks 125
S. Prabhu
B.K. Vinayagam

An Experimental and Theoretical Analysis of Projectile and Target Geometry Effects on Ballistic Limit Velocity

M. Amiri

Research Institute of Petroleum Industry, Tehran, Iran

*amirimm@ripi.ir

ABSTRACT

FRP (Fibre Reinforce Plastics) laminates are now widely used in different industries like aviation, marine and transportation as FRP has shown considerable strength and hardness. However, these materials are vulnerable to lateral intensive static loads and impacts but have proved a good stability and strength in industrial applications. In this paper, an analytical method for ballistic impact on FRP laminates has been proposed along with impact analysis of the panel, which has been carried out in two stages; Rupture and Wave-dominated local failure. First a simple analytical model for local deformation failure and critical shear failure has been used to predict perforation in FRP laminates. For verification of the model, several projectile impact experiments have been conducted to evaluate proposed model. It is concluded that experimental data are in good agreement with proposed analytical model results and effects of different geometrical parameters like panel dimensions and projectile diameter on ballistic velocity have been studied. In addition, analytical data have also been verified with results which were obtained from of LS-DYNA simulation.

Keywords: *Fibre-Reinforced Plastic, Impact, Failure Analysis, Ballistic Limit Velocity.*

Introduction

Fibre-reinforced plastic (FRP) is a one type of composite materials which made of a polymer matrix reinforced with fibres. The commonly used fibres are glass, aramid or carbon. Some other fibres like paper or wood or asbestos have been rarely used and the resin usually consist of an epoxy, vinylester or polyester thermosetting plastic. Aziz has studied the ballistic impact study for the non-filled aluminium tank. The results showed that the ballistic limit for the front tank wall and rear tank wall was 257.7 m/s and 481 m/s, respectively. In addition, this study presented the correlation of the impact velocity towards residual velocity, damage area, wall deflection, velocity drop and energy absorbed [1]. Yunus has investigated, the effect of low energy impact to the residual strength and modulus of short kenaf fibre reinforced epoxy composites. He found that the low energy impacts were affecting the residual strength and residual stiffness which indicated the short kenaf fibre reinforced epoxy composites were extremely sensitive to the impact loads. The damages were manifest by the visible observation of cracks on the specimens [2]. Gu [3] has presented an analytical model of projectile penetration in composite materials which based on adsorbed energy by fibres regarding strain effect on stress-strain relation in fibres. He has modelled a woven fibre instead of a composite material. Gellert [4] obtained ballistic limit velocity on Glass Fiber Reinforced Plastic (GFRP) laminates with different thickness, under projectile impact on conic head. Ulven [5] has experimentally studied effect of projectile head shape on perforation ballistic limit and energy adsorption VARTM carbon/epoxy composite panels.

Modelling and Analysis

There are two steps that have been considered for impact analysis on FRP laminates. Complete deformation with local fragmentation and local deformation are caused by wave. First of all, an analytical model is proposed for complete laminate deformation which subjected to flat head projectile impact. This model goes with shear failure criteria which could be used to predict laminate perforation. By combining local failure model of the governing wave and general concept of critical impact velocity theory (Von Karman) second fracture mode will be gained. Assuming a predefined value for local notch, overall bending, energy adsorption and neglecting

energy losses like friction an analytical model for impact between flat head projectile and thin FRP laminates has been developed.

Semi static force and displacement

In Figure 1, a FRP laminate which is statically loaded with a flat projectile is shown. In the Figure 1 equivalent spring system is represented. Relation between semi static contact force P with local notch is as below [6,7]:

$$P = K_c \alpha \quad (1)$$

Where:

$$K_c = \frac{2R}{\pi H_0} \text{ is contacting hardness;}$$

R : Projectile Radius;

And H_0 is obtained from following [6,7]:

$$H_0 = \frac{(\gamma_1 + \gamma_2)C_{11}}{2\pi(C_{11}C_{33} - C_{13}^2)},$$

$$Q = (C_{11}C_{33} - C_{13}^2 - 2C_{13}C_{44})/2C_{11}C_{44}$$

$$\gamma_{1,2}^2 = Q \pm \sqrt{Q^2 - C_{33}/C_{11}}$$

Where C_{ij} is the ‘‘Elastic Constants’’ for isotropic elastic material.

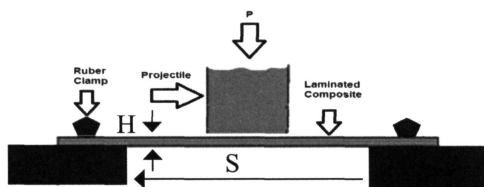


Figure 1: Laminated plate encountering a flat head projectile impact

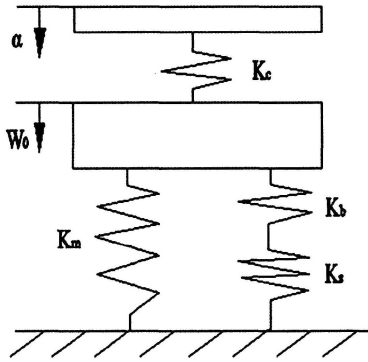


Figure 2: Impact spring model

$$P = K_{bs} W_0 + K_m W_0^3 \quad (2)$$

Where:

W_0 : is vertical deflection of mid plane

K_{bs} : is shear and bending effective stiffness

K_{bs} : is effective shell stiffness for fixed plates.

K_m and K_b for fixed plates are obtained from following relations [8,9]:

$$K_b = \frac{16\pi E_1 H^3}{3(1-\nu_{12}^2)S^2} \quad (3)$$

$$K_m = \frac{191\pi E_1 H}{162S^2} \quad (4)$$

$$K_{bs} = \frac{K_b K_s}{K_b + K_s} \quad (5)$$

In the above relations, S is the laminate plate dimension. Effective shear stiffness is obtained from following relation [8]:

$$K_s = \frac{4\pi}{3} G_{13} H \left(\frac{E_1}{E_1 - 4\nu_{12} G_{13}} \right) \left(\frac{4}{3} + \text{Log} \frac{S}{2R} \right)^{-1} \quad (6)$$

Energy Adsorption

Adsorbed energy in laminate is considered as a total deformation energy, failure energy and delamination energy. Wasted energy caused by deformation is equal to sum of contact energy (E_{ct}) and adsorbed energy by complete deformation (E_{bm}). Consequently, by replacing W_{of} (critical vertical deflection) with W_o deformation energy is obtained as below:

$$E_{df} = E_{\alpha} + E_{bm} = \int_0^{\alpha} Pd\alpha + \int_0^w PdW_o = \frac{(K_{bs}W_{of} + K_m W_{of}^3)^2}{2K_c} + \frac{1}{2}K_{bs}W_{of}^2 + \frac{1}{4}K_m W_{of}^4 \quad (7)$$

By the aid of following approximation deformation energy is obtained [6].

$$P = K_{bs}W_{of} + K_m W_{of}^3 = 2\pi RHK\tau_{13} \quad (8)$$

τ_{13} is vertical laminate shear strength and $2K$ being fixture factor [6]. In this paper we consider $2K$. By considering ϕ as an experimental constant, adsorbed energy from failure for $H/D > \phi$ is obtained by following equation:

$$E_{fac} = \pi R^2(H - \phi D)e_t + \pi R(\phi D)^2 K \tau_{13} \quad (1-9)$$

And for:

$$E_{fac} = \pi RH^2 K \tau_{13} \quad (2-9)$$

Where e_t is tensile failure energy density. The value of ϕ is consider 0.21 approximately [10]. Delamination is initiated under contact loading region by forming cracks in inner plane matrix by shear stress. Delamination could propagate through material complying mode 1 (tensile) and mode 2 (compressive). Delamination energy on FRP laminates is stated as below [10]:

$$E_{del} = A_d \times G_{IIc} \quad (10)$$

In the above expression, A_d is delaminating surface on mid plane and G_{IIc} is fracture toughness in second mode [6].

$$E_{del} = \frac{9}{16\pi H^2} \left(\frac{P_d}{\tau_{IRSS}} \right)^2 G_{IIc} \quad (11)$$

$$P_d^2 = \frac{8\pi^2 E_1 H^3 G_{IIc}}{9(1-\nu_{12}^2)} \quad (12)$$

Where P_d is delamination critical force and τ_{IRSS} is internal shear stress. Energy is semi static loading in FRP laminates perforation in flat head projectile is obtained from following equation:

$$E_T = E_{def} + E_{frac} + E_{del} \quad (13)$$

Impact perforation energy (E_p) is stated as below [6]:

$$E_p = \phi E_T \quad (14)$$

Where ϕ is dynamic increment factor which is obtained from following equation:

$$\phi = \begin{cases} 1+B \left(\frac{V_i}{V_c} \right) & (V_i < V_c) \\ 1+B & (V_i > V_c) \end{cases} \quad (15)$$

Where B is experimental constant, V_c is Von Karman critical velocity and V_i is projectile initiate velocity. In this paper ϕ is considered to be 0.21.

$$V_b = \sqrt{\frac{2\phi(E_{def} + E_{frac} + E_{del})}{G}} \quad (16)$$

Local Failure Caused by Wave

Resisting force against flat head projectile while hitting FRP laminates are derived from following equation [18]:

$$F = \frac{\pi D^2}{4} (\sigma_e + \beta \sqrt{\rho_i \sigma_e V_i}) \quad (18)$$

Where σ_e is linear elastic limit for FRP laminates in compression through thickness direction, ρ_i is FRP laminate density and β is experimental constant which is considered for flat head projectile.

By using energy equilibrium, $\frac{1}{2} G V_b^2 = F \cdot H$ and replacing $V_i = V_b$ in which ballistic limit for thick FRP laminates are obtained as below:

$$V_b = \frac{\pi \sqrt{\rho_i \sigma_e} D^2 H}{2G} \left[1 + \sqrt{1 + \frac{2G}{\pi \rho_i D^2 H}} \right] \quad (19)$$

Thickness Evaluation Criterion for FRP Laminates

By using $V_b = V_c$ and replace it in equation (18) and by using $G = \frac{1}{4} \pi D^2 L \rho_p$ in which L is length and ρ_p is projectile density, ratio of FRP laminate critical thickness to projectile diameter is obtained as below:

$$\left(\frac{H}{D} \right)_c = \frac{\varepsilon_f^2}{2 \left[1 + 2 \sqrt{E_i / \sigma_e \varepsilon_f} \right]} \left(\frac{E_i}{\sigma_e} \right) \left(\frac{\rho_p}{\rho_i} \right) \left(\frac{L}{D} \right) \quad (20)$$

In equation (20) if $H/D \geq (H/D)_c$ then FRP laminate will break in local mode caused by wave, otherwise it will be broken in deformation mode by local dividing in two parts.

Results and Discussion

FRP laminates are subjected to flat head projectile as shown in Figure 1. FRP laminates properties are shown in Table 1. Results obtained from proposed model are compared with experimental data which mentioned in references [4,5]. Figure 3 shows values of calculated ballistic limits in term of H/D .

In this figure a comparison have been made between gathered data from experiment analysis and those data which presented in reference [4]. Critical ratio $(H/D)_c$ for GFRP laminates which are subjected to impact from a 3.84 gr and 6.35 mm flat head projectile with the aid of eq. (19) is equal to 0.160.

In Figure 4 a comparison is represented between experimental data in reference [4] and ballistic limit velocity. Critical rate ratio $(H/D)_c$ for CFRP laminates which subjected to flat head projectile which its mass is 14 gr and diameter 12.7 mm by using equation (24) is equal to 0.199.

Table 1: Material properties
Carbon Epoxy E-Galss/Vinylester [4,5]

S	100 mm	101.6mm
ρ_t	1850 Kg/m ³	1550 Kg/m ³
	24.9 GPa	53.7GPa
E_3	7.4 GPa	11.7GPa
G_{13}	1.9 GPa	4GPa
ν_{12}	0.15	0.31
τ_{13}	49MPa	79MPa
ε_f	0.021	0.0138
τ_{IRSS}	13 MPa	50MPa
e_t	4.98 MJ/m ³	5.1 MJ/m ³
G_{IIC}	2.8 KJ/m ²	0.8 KJ/m ²
B	1.64	0
σ_e	250MPa	85MPa

As shown in Figure 3 and Figure 4, local failure model caused by wave are in good agreement with experimental data; however local deformation model, couldn't predict ballistic limit properly. With any increment in plate thickness, difference between experimental results and prediction of local deformation model become more noticeable.

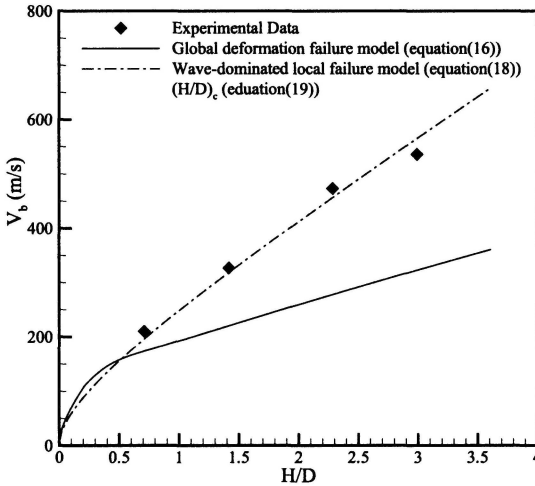


Figure 3: Comparison between ballistic limit velocity obtained from represented model and experimental data in reference [4]

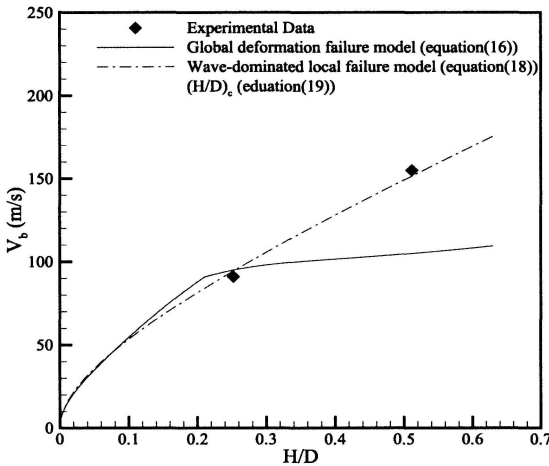


Figure 4: Comparison between ballistic limit velocity obtained from represented model and experimental data in reference [5]

In the next step effect of plate dimensions and projectile diameter on ballistic limit was investigated. Figure 5 shows variation in ballistic limit velocity with a carbon/epoxy E-Glass/vinylester plate dimensions. Laminate plates thickness is 2.5 mm which subjected to 14 gr and 12.7 mm diameter flat head projectile. By considering Figure 5 it becomes obvious that in thin plates when dimension increase ballistic limit velocity be higher.

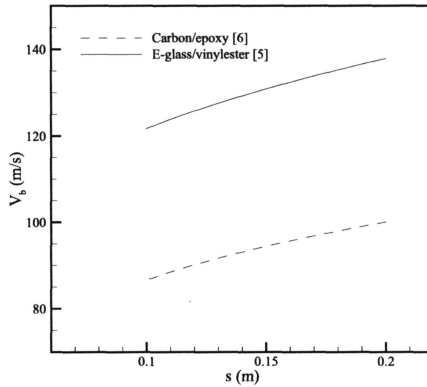


Figure 5: Plate dimension effect on ballistic limit velocity for E-glass/vinylester

Figure 6 shows ballistic limit variation to projectile diameter for 3.2 mm thick epoxy/carbon laminate. Projectile mass is 14 gr which its length varies with diameter variation. With any increment in projectile diameter predicted ballistic limit velocity will increase.

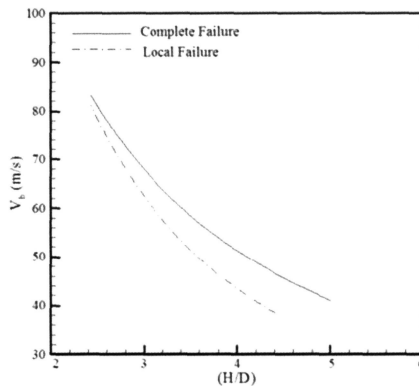


Figure 6: Ballistic limit velocity varies with changes in plate thickness to projectile diameter ratio for epoxy/carbon.

As the analytical model is in good agreement with experimental results, ballistic velocity for materials listed in Table 2 is now calculated and be compared with software results.

Table 2: Projectile mechanical characteristics

$\rho \left(\frac{Kg}{m^3} \right)$	$E \text{ (GPa)}$	ν
7830	207	0.28

Table 3, 4, 5 and 6 represent Epoxy-Carbon Elastic properties, E-glass/epoxy Elastic properties, Epoxy-Carbon strength properties and Analysis E-glass/epoxy strength properties which were used in ANSYS/LS-DYNA modelling setup.

Table 3: Epoxy-carbon elastic properties in software modeling setup

$E_{11} \text{ (GPa)}$	$E_{22} \text{ (GPa)}$	$E_{33} \text{ (GPa)}$	$E_{12} \text{ (GPa)}$	$E_{13} \text{ (GPa)}$	$E_{23} \text{ (GPa)}$	V_{12}	V_{13}	V_{23}	$\rho \left(\frac{Kg}{m^3} \right)$
52.1	52.1	8	3.89	3.8	3.8	0.045	0.064	0.064	1306

Table 4: E-glass/epoxy elastic properties in software analysis

$E_{11} \text{ (GPa)}$	$E_{22} \text{ (GPa)}$	$E_{33} \text{ (GPa)}$	$E_{12} \text{ (GPa)}$	$E_{13} \text{ (GPa)}$	$E_{23} \text{ (GPa)}$	V_{12}	V_{13}	V_{23}	$\rho \left(\frac{Kg}{m^3} \right)$
21.15	21.16	8.3	3.99	4.1	4.1	0.169	0.270	0.276	1750

Table 5: Epoxy-carbon strength properties in software analysis

$X_T \text{ (MPa)}$	$Y_T \text{ (MPa)}$	$Z_T \text{ (MPa)}$	$S_{12} \text{ (MPa)}$	$S_{13} \text{ (MPa)}$	$S_{23} \text{ (MPa)}$	$X_C \text{ (MPa)}$	$Y_C \text{ (MPa)}$	$Z_C \text{ (MPa)}$
545	545	48.5	64	64	64	410	410	210

Table 6: E-glass/epoxy strength properties in software analysis

$X_T \text{ (MPa)}$	$Y_T \text{ (MPa)}$	$Z_T \text{ (MPa)}$	$S_{12} \text{ (MPa)}$	$S_{13} \text{ (MPa)}$	$S_{23} \text{ (MPa)}$	$X_C \text{ (MPa)}$	$Y_C \text{ (MPa)}$	$Z_C \text{ (MPa)}$
213	213	26.2	26	26	26	220	220	130

The model which was created in ANSYS/LS-DYNA is bilinear isotropic solid with SHELL181 element. Elements contact are TARGE170 and CONTA173 with friction coefficient MU=0.3. Figures 7, 8 and 9 represent finite element modelling in ANSYS/LS-DYNA software.

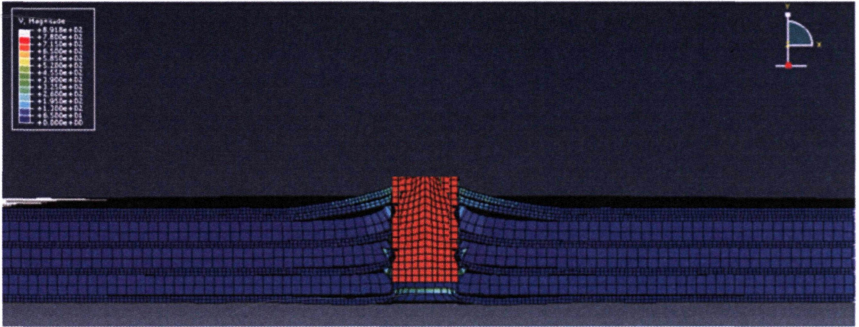


Figure 7: Projectile and epoxy-carbon composite with thickness of 3.2 mm perforated by projectile

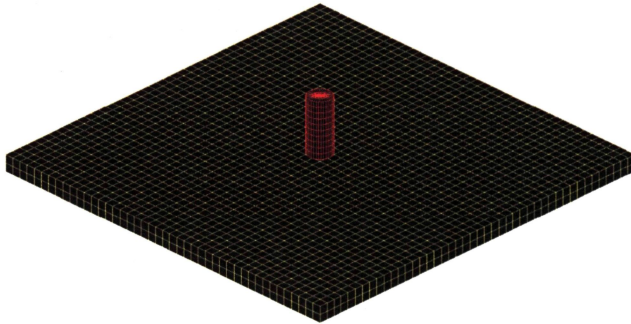


Figure 8: Projectile and 4.5 mm E-glass/epoxy composite laminates before strike

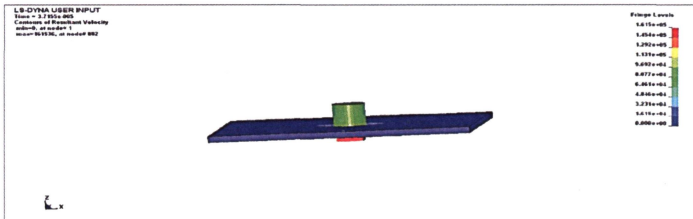


Figure 9: 4.5 mm thick E-glass/epoxy laminate perforated by a projectile

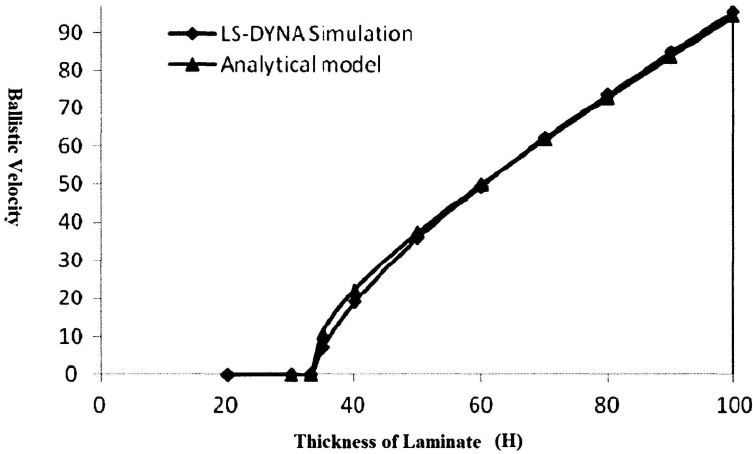


Figure 10: A Comparison between ballistic limit velocity results from analytical model and software simulation for carbon-epoxy

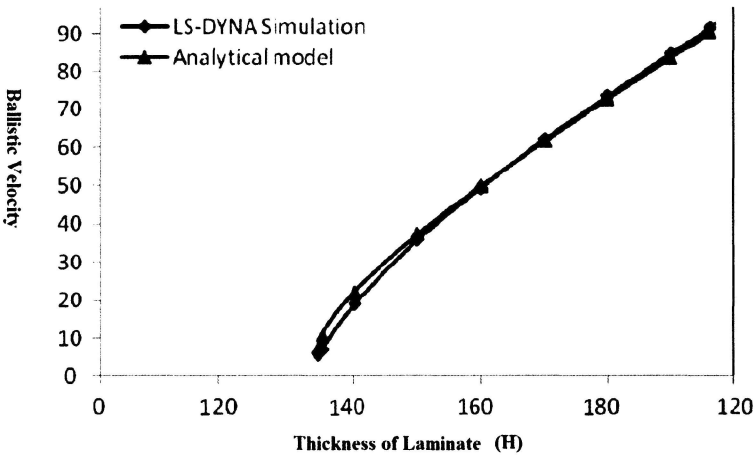


Figure 11: A Comparison between ballistic limit velocity results from analytical model and software simulation for E-glass/epoxy

As it is shown in Figure 10 and Figure 11 there is a little difference between analytical results and software simulation results. The main reason for such a difference comes from not considering Delamination Energy in software solution. Laminates has been modeled by ANSYS/LS-DYNA. The results show that with incretion in laminate thickness, ballistic limit velocity will also increase.

Conclusion

In this paper, ballistic limit velocity and perforation in fibre reinforced plastic laminates subjected to strike were investigated. Two main category of failure have been studied; the first one is complete deformation with centralized failure and the second one is local failure which was caused by wave. In presenting analytical model for complete deformation, semi-static method have been employed to estimate the absorbed energy. Moreover; mechanical increment factor has been used for calculating perforation energy. By combining Von Karman critical velocity method with local failure model for governing wave, the second failure mode was gained. Theoretical results for ballistic limit wave prediction are in good agreement with experimental results. Presented analytical model is simple and agrees with experimental results. By means of proposed model it could be concluded that when plate dimensions and projectile diameter increase ballistic limit velocity will also increase. Future research should focus on different shapes of projectile when encountering a target with different kind of materials.

References

- [1] Aziz, MR., Kuntjoro, W., David, NV., and Ahmad, R. "Ballistic Resistance Analysis of Non Filled Tank against Fragment Simulating Projectile (FSP)", *Journal of Mechanical Engineering*, Vol.10, No.2, 79-95, 2013.
- [2] Yunus, S. A., Abdullah, N., Abdul Halim, Salleh, Z., and Taib, Y. "Low Energy Impact on the Short Kenaf Fibre Reinforced Epoxy Composites: Effect to the Residual Strength and Modulus", *Journal of Mechanical Engineering*, Vol. 12, No. 2, 71-84, 2015.
- [3] Hoo Fatt, MS., and CF. Lin. "Perforation of clamped woven E-glass/polyester panels". *Composites Part B*, 35(5), pp. 359–378, 2004.
- [4] Gu, B. "Analytical modeling for the ballistic perforation of planar plain woven fabric target by projectile", *Composites (Part B)*, 34(4), pp. 361-371, 2003.
- [5] Gellert, EP, Cimpoeru, SJ., and Woodward, RL. "A study of the effect of target thickness on the ballistic perforation of glass–fibre-reinforced plastic composites", *Int. Journal Impact Eng.*, 24(5), (2000) pp. 445–456.
- [6] Ulven, C. Vaidya, UK. Hosur, MV. "Effect of projectile shape during ballistic perforation of VARTM carbon/epoxy composite panels", *Composite Structure*, 61(1–2), (2003) pp.143–150.

- [7] Wen, HM. Reddy, TY. Reid, SR. "Soden PD. Indentation, penetration and perforation of composite laminates and sandwich panels under quasi-static and projectile loading", *Key Eng. Mater.* pp 141–143:501–552, 1998.
- [8] Fabrikant, VI, Selvadurai, APS., Xistris, GD. "Asymmetric problem of loading under a smooth punch", *J Appl Mech.*, 52(3), (1985) pp 681–685.
- [9] Shivakumar, KN. Elber W., and Illg W. "Prediction of impact force and duration due to low velocity impact on circular composite laminates", *Journal Applied Mechanics*, 52(3), pp. 674–680, 1985.
- [10] Timonshenko, SP., and Woinowsky-Krieger, S. "Theory of plates and shells", McGraw Hill, New York, 1961.
- [11] Qin Y. "Theoretical and numerical study on failure modes of FRP laminates struck normally by projectiles", MSC Dissertation, University of Science and Technology of China, 2009.
- [12] Naik, N.K. Y. Chandra, S. Sailendra, M. "Damage in Woven-fabric composites subjected to low velocity impact", *Composite Science and Technology*, pp. 731-744, 2000.

1	Thin-walled Box Beam Bending Distortion Analytical Analysis <i>A Halim Kadarman, Solehuddin Shuib, Ahmad Yusoff Hassan & Muhammad Adib Izzuddin Ahmad Zahrol</i>	1
2	An Experimental and Theoretical Analysis of Projectile and Target Geometry Effects on Ballistic Limit Velocity <i>M. Amiri</i>	17
3	A Comparative Study of Prediction Techniques for Supersonic Missile Aerodynamic Coefficients <i>Loai A. El-Mahdy, Mahmoud Y. M. Ahmed, Osama K. Mahmoud & Omar E. Abdel-Hameed</i>	33
4	Experimental Investigation on the Influences of Varying Injection Timing on the Performance of a B20 JOME Biodiesel Fueled Diesel Engine <i>S. Jaichandar & K. Annamalai</i>	57
5	Tensile Performance of Half-Lap Timber Nailed Joint Strengthened Using CFRP Sheet <i>Nurain Rosdi, Nik Norhafiza Binti Nik Yahya, Rohana Hassan, Mohd Hanafie Yasin & Nor Jihan Abd Malek</i>	75
6	Surface Roughness and Roundness Optimization on Turning Process of Aluminium Alloy with Taguchi Method <i>Sudjatmiko, Rudy Soenoko, Agus Suprpto & Moch. Agus Choiron</i>	87
7	Numerical Simulation of The Femur Fracture With and Without Prosthesis Under Static Loading Using Extended Finite Element Method (X-FEM) <i>Zagane Mohammed El Sallah, Benbarek smail, Benouis Ali, Sahli Abderahmen, Bachir Bouiaftra bel abbes & Boualem Serier</i>	97
8	Optimization of Robot Plasma Coating Efficiency using Genetic Algorithm and Neural Networks <i>S.Prabhu & B.K.Vinayagam</i>	113